

Study of the flashover occurrence on polluted composite insulators: impact of the relative permittivity of water droplets

Sarah Bendimerad, Hocine Hadi, Mohammed El Amine Abed

Laboratoire de Génie Electrique d'Oran, Université des Sciences et de la Technologie d'Oran Mohamed Boudiaf, USTO-MB,
BP 1505, El M'naouer, 31000 Oran Algérie
E-mail: sarah.bendimerad@univ-usto.dz

Abstract. The presence of water droplets on the surface of composite insulators greatly increases the electric-field intensity in their vicinity. The aim of the paper is to contribute to the understanding of the flashover phenomenon occurring in composite insulators. The flashover voltage (FOV) is measured by taking into account the electrical conductivity and relative permittivity of the various liquids used and the voltage regime. The correlation between the number of the flashover shocks, the surface current and the hydrophobicity is investigated. To validate and explain the experimental results, the electric field is numerically calculated using the Comsol Multiphysics software. Experimental results show that FOV varies as a function of the electrode polarity, conductivity and relative permittivity of the liquids used and the regime of voltage. The calculation results, show that the contact angle (CA) and permittivity significantly affect the electric field. However, the most determining factor for FOV is the relative permittivity.

Keywords: Flashover voltage (FOV), Water droplet, Contact angle (CA), Relative permittivity, Electric field.

Študija pojava preboja na onesnaženih kompozitnih izolatorjih: vpliv relativne prepustnosti vodnih kapljic

Prisotnost vodnih kapljic na površini kompozitnih izolatorjev močno poveča jakost električnega polja v njihovi bližini. Namen prispevka je prispevati k razumevanju pojava preboja, ki se pojavlja v kompozitnih izolatorjih. Napetost preskoka (FOV) se meri ob upoštevanju električne prevodnosti in relativne prepustnosti različnih uporabljenih tekočin ter napetostnega režima. Raziskali smo korelacijo med številom udarnih sunkov, površinskim tokom in hidrofobnostjo. Za potrditev in razlago eksperimentalnih rezultatov smo električno polje numerično izračunali s programsko opremo Comsol Multiphysics. Eksperimentalni rezultati kažejo, da se FOV spreminja v odvisnosti od polarnosti elektrode, prevodnosti in relativne prepustnosti uporabljenih tekočin ter režima napetosti. Rezultati izračuna potrjujejo, da kontaktni kot (CA) in prepustnost pomembno vplivata na električno polje.

1 INTRODUCTION

In recent years, composite insulators have been increasingly used in high-voltage overhead lines due to the many advantages they offer over the traditional ones, most notably their hydrophobicity that prevents the formation of a continuous water film on their surface. However, the presence of water droplets on the surface of composite insulators leads to a local increase in the electric-field value (due to their relative

permittivity [1]-[3]) at the triple contact point (θ) formed by the insulator, the droplet and air (Fig. 1), this can initiate partial surface discharges that may be developing until the flashover occurrence.

The flashover phenomenon occurring in polluted composite insulators in presence of water droplets is widely studied [3]-[7]. Some researchers particularly focused on the impacting parameters, such as the shape of the applied voltage and the size, volume, number and conductivity of water droplets [8]-[13].

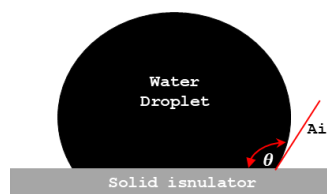


Figure 1. CA of a water droplet.

The (CA) (θ) is a very important indicator of the surface hydrophobicity. Its role in the electric-field distortion and initiation of partial discharges on the insulator surface is widely investigated [4], [13]-[17].while, the interaction between the relative permittivity of the droplet and the dielectric strength on the insulator surface still remains to be studied.

The paper reviews the knowledge acquired so far on the flashover phenomenon occurring in composite insulators in a dry and clean state and in the presence of a shaped droplet pollution deposit. The effect of the pollution relative permittivity is investigated and the electric-field distribution on the insulator surface is numerically calculated using the finite- element method (FEM) with the Comsol Multiphysics software.

2 EXPERIMENTAL SET-UP

Our measurements are carried out at the laboratory of High- Voltage and Electrical Discharges of the USTO-MB University. The laboratory high -voltage test room is composed of two platforms see (Fig. 2).

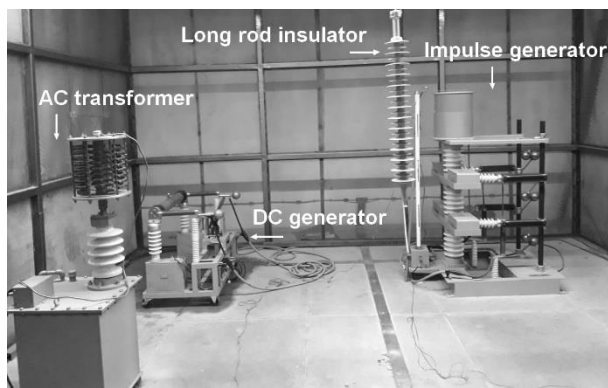


Figure 2. Laboratory test station.

2.1 Voltage sources

Three high-voltage sources are used: an alternating voltage (AC) generator and a direct voltage (DC) generator, both of the positive and negative polarity, and an impulse voltage generator of a positive and negative polarity:

- a 5 kVA, 220V/50 kV AC voltage generator;
- a 0÷70 (kV), 0÷30 (mA) DC voltage generator;
- a 170 kV, 1.2/50 μ s (lightning type) Impulse voltage generator.

2.2 Surface current measurement

The surface current is measured on the insulator surface between the guard and the ring electrode using a three-electrode system (Fig. 3) compliably with the IEC 93 standard. The guard electrode serves as a protection electrode to shunt the insulator bulk current outside the electrometer. The DC surface current measurement setup can be found in [18].

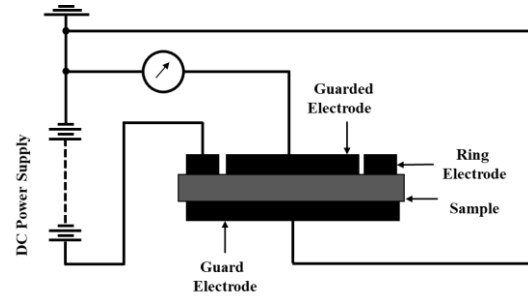
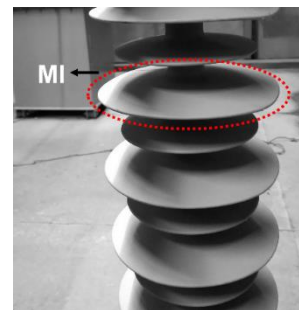


Figure 3. Surface current measurement setup.

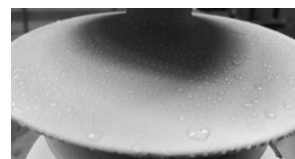
2.3 Studied models, techniques and experimental procedures

2.3.1 Insulator model I (MI)

The MI insulator is a single shed (the large shed) of a silicone rubber insulator chain whose two ends (top and bottom) are supplied by a test voltage source (Fig. 4 (a)). The FOV of the unpolluted insulator (clean state) is recorded. The pollution is deposited on the insulator either with a spray nozzle, providing an uncontrolled (non-uniform) pollution deposit (Fig. 4 (b)), or with a micropipette, providing a uniform deposit of 30 droplets (Fig. 4 (c)), then the FOV is measured. After that the insulator is left to rest for a period of about twenty minutes to recover its hydrophobicity [19]. After that, FOV is measured. Then the test is repeated.



(a)



(b)



(c)

Figure 4. (a) MI insulator, and the applied pollution methods: (b) spray method, (c) droplet- deposition method.

2.3.2 Insulator model II (MII)

The tests are performed on silicone samples of a 40mm diameter and of an average thickness of 4.7mm. The samples are cut from an insulator chain. The voltage is applied between, a grounded electrode (flat electrode), and a half- spherical electrode of a radius of 4.5mm

from which, the High DC voltage is applied. The electrodes are spaced 1mm apart (Fig. 5).

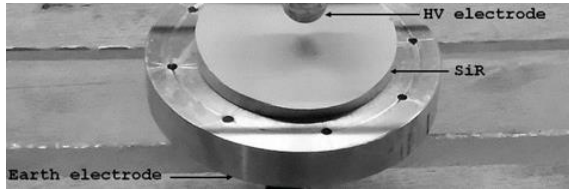


Figure 5. MII insulator.

FOV used in our study is the mean values of several tests with a twenty-minute pause interval between two successive tests.

2.4 Permittivities and conductivities of the insulating liquids used

The following parameters directly affecting FOV are studied: the permittivity and conductivity of the insulating liquid droplets (distilled water, glycerine and oil) and the type of the applied voltage.

At each test performed in the presence of droplets on the insulator surface and for each liquid used, the droplet volume is kept constant at 10 μ l. The insulating liquid conductivity and relative permittivity values used in our experiments are given in the Table 1.

Table 1. Properties of the water droplets used for the MII insulator FOV study.

Liquid	Conductivity [μ S/cm]	Relative Permittivity	CA
Oil	0.1	2	39°
Glycerin	0.3	42	66°
Distilled water	2.4	80	97°

3 RESULTS AND DISCUSSION

3.1 Polluted insulator

3.1.1 Pollution conductivity impact on FOV

To evaluate the impact of the pollution conductivity on the MI insulator FOV, a salt solution of several conductivity levels is used by dissolving sodium chloride (NaCl) in distilled water with the conductivity of 2.4 μ S/cm.

Fig. 6 shows the FOV variation at different voltage regimes as a function of the conductivity of the pollution deposit sprayed on the insulator surface.

At any voltage regime, FOV decreases with the increase in the pollution layer conductivity. FOV at a pulse regime is minimally by 40% higher than any other voltage regime. Except for the distilled water with an invariable FOV, FOV in the negative polarity is higher than in the positive polarity.

Fig. 7 shows the FOV variation at AC as a function of the pollution deposit conductivity (droplets) on the insulator surface. The presence of droplets on the insulator any surface decreases the FOV by 42% compared to the clean case. Fig. 6 shows that FOV decreases with an increase in the droplet conductivity, as also reported in [8], [9], [11], [20] and, that the conductivity effect on FOV significantly increases between 35 and 130 μ S/cm.

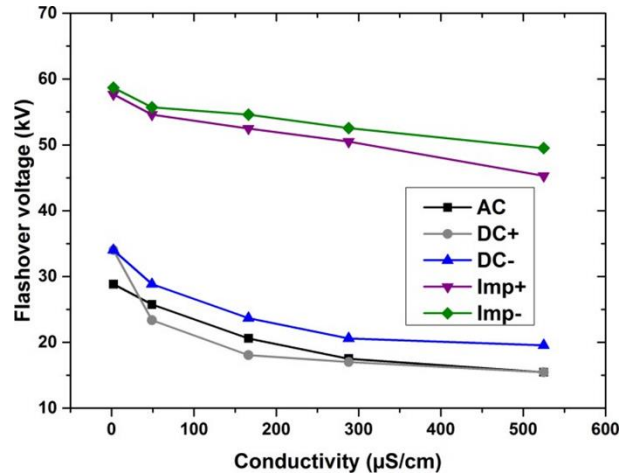


Figure 6. FOV as a function of the conductivity of the pollution deposit (spray) on the MI insulator surface.

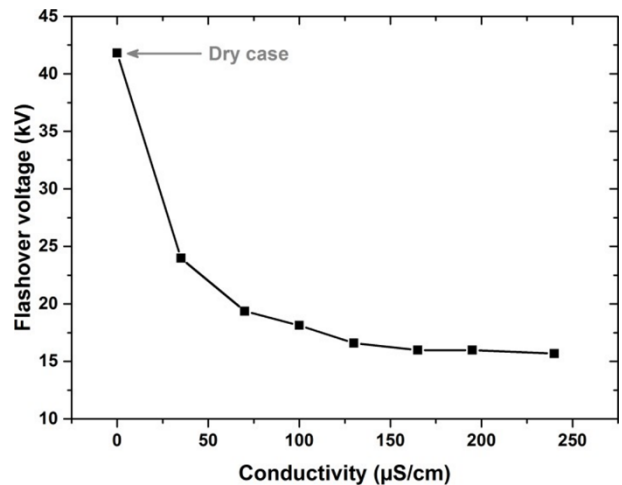


Figure 7. FOV versus the conductivity of the controlled droplet deposition on the MI insulator surface.

Figs. 6 and 7 show that irrespective of the used deposition method the relationship between FOV and the pollutant conductivity is the same.

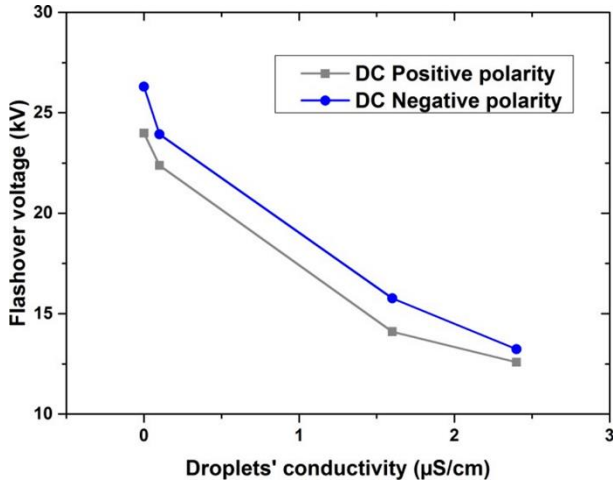


Figure 8. FOV versus the conductivity of a controlled droplet deposition on the MII insulator surface.

Fig. 8 shows the variation in DC FOV (positive and negative polarity) as a function of the droplet conductivity on the MII insulator surface. The conductivity and polarity impact on FOV is the same as in figures 6 and 7, meaning that the MII insulator model reproduces very well the results obtained for the real insulator, and will therefore, be used also for the rest of the tests.

3.1.2 The impact of the pollution relative permittivity on FOV

Fig. 9 shows the FOV variation as a function of the droplet deposit permittivity on the MII insulator surface. Generally, FOV decreases with an increasing droplet relative permittivity [21]. There are three distinct parts in the trend curve. First, FOV drops when the relative permittivity changes from 1 to 2 due to the increased electric-field as a result of the liquid change (presence of droplets) [13]. Second, when the relative permittivity is between 2 and 40, the voltage continues to decrease slightly. Third, there is a significant decrease in FOV when the relative permittivity is between 40 and 80.

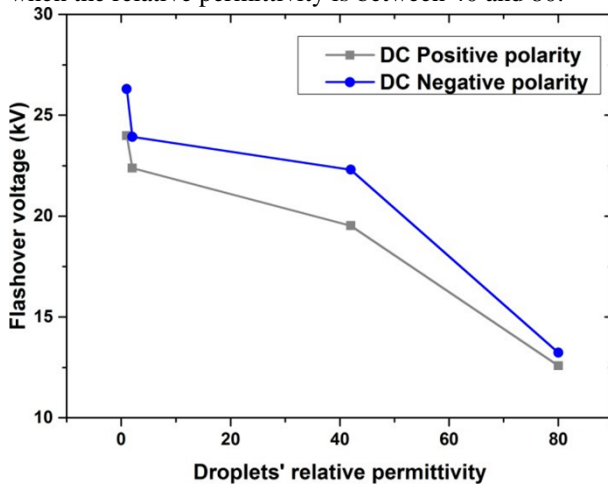


Figure 9. FOV versus the relative permittivity of the controlled droplet deposition on MII insulator surface.

3.1.3 CA impact on FOV

Besides the electrical properties of the droplet deposit, CA also affects the insulator dielectric strength [22]-[24]. Fig. 10 shows the CA variation as a function of the relative permittivity of the liquids used and a linear dependence between these two properties.

As also reported in [11] and [25], increasing CA of droplets deposited on the composite insulator surface increases its FOV due to of the reduced electric field at the triple-contact point, i.e., air, insulator and liquid.

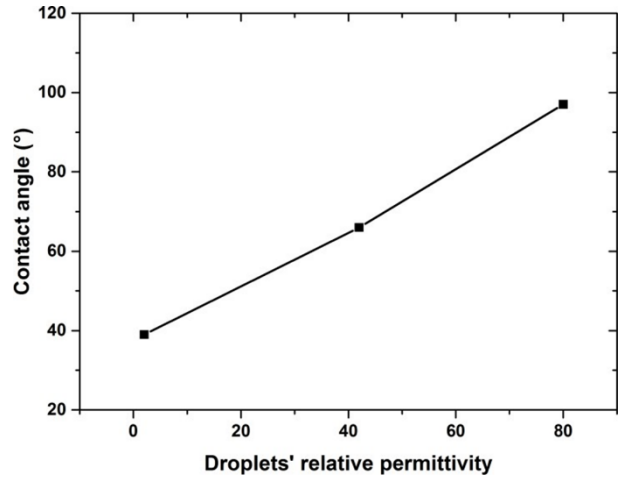


Figure 10. CA versus the controlled droplet deposition permittivity on a real insulator surface.

This is note in line with Figs. 9 and 10 where FOV decreases with CA increasing. This raises the question about the contribution of the permittivity and the CA impact on the FOV decrease.

A parametric study of the permittivity and CA effect on the electric-field distribution on the insulator surface (the MII model) in the presence of a water droplet is made.

3.2 Analysis of the electric field on the (MII) insulator surface

The 3D electric field is numerically calculated using the finite-element method with the COMSOL Multi-physics software. The AC/DC module of the COMSOL Multi-physics is used.

The intensity and distribution of the electric field on the insulator surface in the presence of droplets with different permittivity values is studied. The II model is reproduced and droplets of different CA values are added (Fig. 11 (b)). Each value corresponds to the nature of the liquid given in Table1.

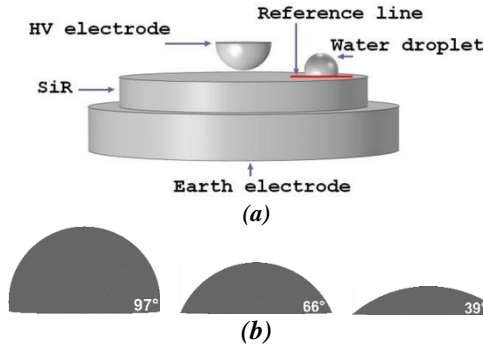


Figure 11. Geometry reproduced on COMSOL Multiphysics: (a) MII model, (b) droplet CA values.

CA is measured in several positions on the insulator surface complying with the recommendations of the IEC62073 standard [26] by depositing 20 μl of a distilled water droplet on the insulator surface.

The droplet picture is taken with a high-resolution camera and then transferred to a computer to determine the CA value using contour analysis software.

3.3 The impact of the droplet parameters on the electric-field distribution and its intensification at the triple-contact point: air, insulation and liquid

3.3.1 The impact of the CA droplet

Fig. 12 (a) shows the variation in the electric field strength on the insulator surface as a function of the droplet CA value. It is shown that the presence of droplets increases the electric field strength at droplet triple-contact point. At the center of the droplet, the electric field value decreases considerably due to the constant electric potential (see Fig. 12 (b)).

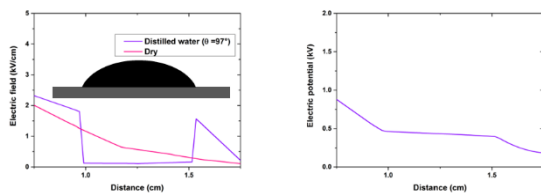


Figure 12. Electric field (a) and electric potential (b) in the presence of a droplet deposited on the insulator surface (MII).

To quantify the intensification of the electric field caused by the droplet on the insulator surface, the ratio between the maximum electric-field value at triple contact point E_{max} and the electric field value in the absence of droplet E_0 is usually used [13]-[15], [27].

The ratio is given by the intensification factor IF :

$$IF = \frac{E_{\text{max}}}{E_0} \quad (1)$$

Fig. 13 shows that with a CA increase IF decreases [13], [15], [16], [28]-[30].

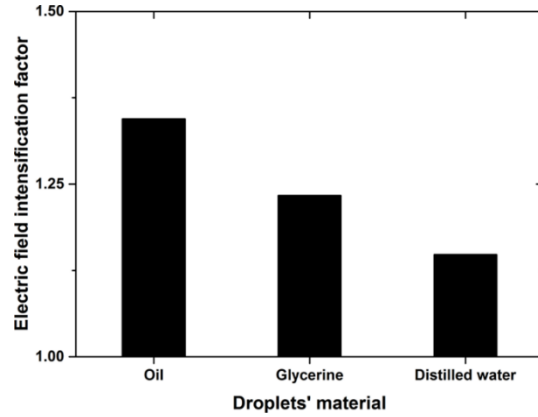


Figure 13. IF as a function of CA corresponding to the liquid of a droplet deposited on the insulator surface.

3.3.2 The impact of the droplet relative permittivity

Fig. 14 shows the variation in the electric-field strength as a function of the droplet relative permittivity. The electric-field strength increases with the increase in the droplet permittivity.

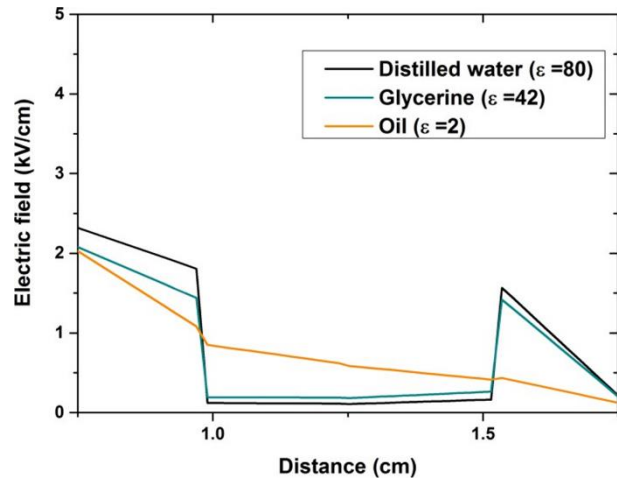


Figure 14. Electric field strength as a function of the relative permittivity of a droplet deposited on the insulator surface.

3.3.3 The CA impact and the droplet relative permittivity

Fig. 15 presents the impact of the permittivity and CA on the electric field strength value on the insulator surface. Which strongly resembles the one in Fig. 14. To be noted, according to Fig. 13, the oil droplet IF is usually higher than that of glycerine and the water droplets. However, in this case the water droplet factor in high as in the case of the FOV measurements results reported in section 3.1.2 (Fig. 9). This also shows that the relative permittivity is the most impacting parameter for a flashover occurrence on a water droplet-polluted insulator. The CA impact plays a secondary role.

To understand the permittivity impact on FOV, it should be noted that the resistive current value of each of the

liquids used is the same and only the contribution of the capacitive current given by expression (2) should be considered:

$$I_s = C \frac{dv}{dt} \quad (2)$$

$$C \propto I_s \quad (3)$$

For the studied MII insulator model (Fig. 11 (a)), the tangential component of the electric field is more significant than the normal component. Irrespective of the contribution of the latter, the droplet and the solid silicone insulator can be assumed as two electric capacitances connected in parallel:

$$C = \epsilon_0 \epsilon_r \frac{s}{d} \quad (4)$$

where ϵ_0 , ϵ_r , s and d are the vacuum permittivity, relative permittivity (of the droplet or solid insulator), surface and diameter of the droplet and/or solid insulator, respectively.

Capacity C_g of the droplet varies depending on the liquid used (distilled water, glycerine and oil) and therefore with the relative permittivity of the droplet and its diameter. The capacity of solid insulator C_{iso} is constant. The expression of equivalent capacity C_{eq} (between the droplet and the solid insulator) (ϵ_{rg} is the relative permittivity of the droplet) is:

$$C_{eq} = C_g + C_{iso} \quad (5)$$

$$C_{eq} \propto \epsilon_{rg} \quad (6)$$

Following the above, the total capacity mostly depends on the droplet relative permittivity when the geometrical shape of the droplet (its diameter) is kept constant as is the case with the numerical simulation (section 3.3.2).

The leakage current measured just before the flashover occurrence is inversely proportional to FOV [19]. By the analogy with Equation (2), the relative permittivity is inversely proportional to FOV.

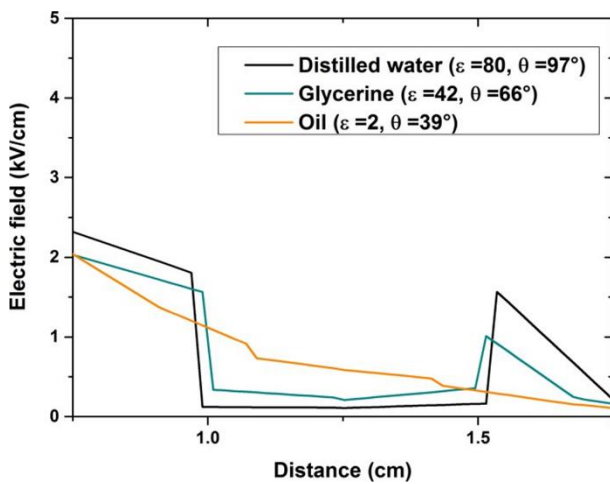


Figure 15. Electric field as a function of CA and relative permittivity of the droplet deposited on the insulator surface.

3.4 Dry and clean insulator

In this section, we will study the impact of the flashover on the surface properties of the MII composite insulator model, such as its hydrophobicity and surface current.

During the process that leads to the flashover of composite insulators, partial discharges are initiated at triple-contact point (metal fitting/air/solid insulator) then elongated according to certain mechanisms. It has been reported that the flashover arc consumes some of the low molecular weight (LMW) of the polydimethylsiloxane (PDMS) species on the insulator surface that are responsible for the material hydrophobicity [31]. This is probably the reason why the hydrophobicity of the insulator decreases at an flashover arc occurrence on its surface (see Fig. 16)

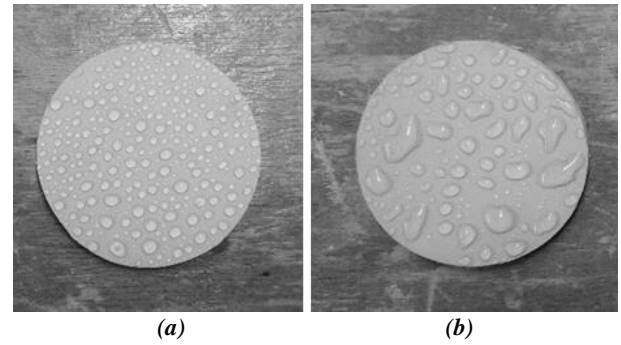


Figure 16. Hydrophobicity of insulator: (a) hydrophobic case, (b) hydrophilic case (after a flashover occurrence).

Fig. 17 shows the variation in insulator FOV as a function of the number of flashover shocks. As in Figs 6, 8 and 9, FOV in the negative polarity is always higher than in the positive polarity. In the negative polarity, FOV decreases only by 7% between 10 and 50 flashover shocks, while in the positive polarity, it decreases any some 14%.

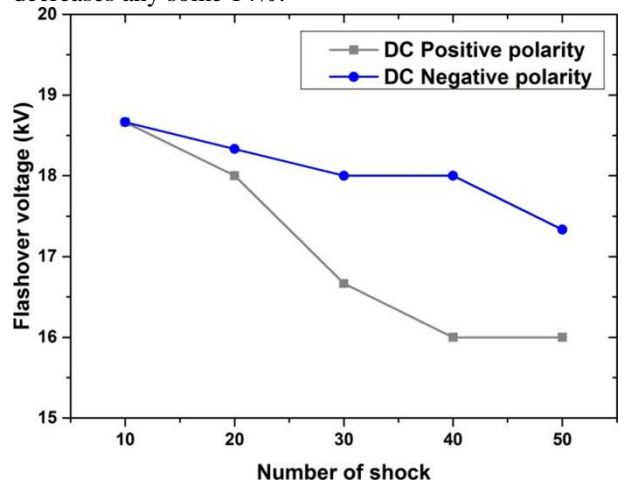


Figure 17. FOV as a function of the number of the flashover shocks.

Fig. 18, shows the variation in the surface current measured on the insulator surface as a function of the number of the flashover shocks. The current increases with the number of the flashover of both polarities, more so in the positive polarity than in the negative one. This is probably due to the density of the electric charges involved during the flashover. The variation in the surface current follows the exponential function given by Equation 7, where I_0 , A and R_0 are constants, and n is the number of the flashover shocks. Table 2 presents the fitting parameters of the obtained curves where R^2 is the correlation coefficient.

$$I = I_0 + Ae^{R_0 n} \quad (7)$$

Table 2. Fitting parameters of the surface current curves as a function of the number of the flashover shocks.

	I_0	A	R_0	R^2
Positive polarity	$1,969.10^{-7}$	$2,070.10^{-9}$	0,145	0,967
Negative polarity	$-3,466.10^{-7}$	$2,971.10^{-7}$	0,016	0,929

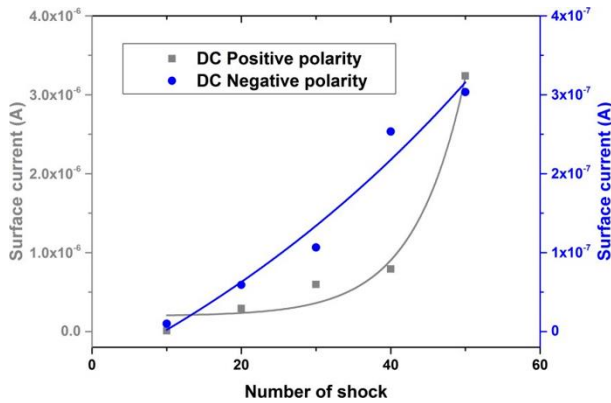


Figure 18. Surface current as a function of the number of the flashover shocks.

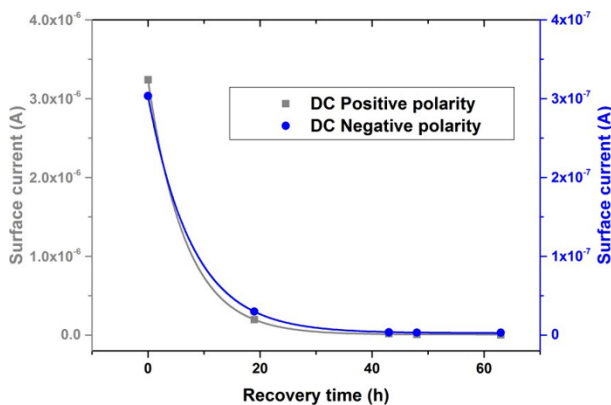


Figure 19. Surface current versus the recovery time after 50 flashover shocks.

Fig. 19 shows the time evolution, of the surface current measured after 50 flashover shocks. Equation 8 shows

the trend of the curves with a correlation coefficient close to 1 (see Table 3) where t is the time and I_0 , A and R_0 are the constants. The decrease in the surface current as a function of the time is normally due to the dissipation of the electric charges accumulated on the insulator surface as a result of the flashover shocks.

$$I = I_0 + Ae^{R_0 t} \quad (8)$$

Table 3. Fitting parameters of the surface current curves as a function of the recovery time after 50 flashover shocks.

	I_0	A	R_0	R^2
Positive polarity	$6,747.10^{-9}$	$3,233.10^{-6}$	-0,149	0,999
Negative polarity	$2,629.10^{-9}$	$3,007.10^{-7}$	-0,126	1

The decrease in FOV shown in Fig. 17 is attributed to of electric charges on the insulator surface after the flashover occurrence. Their density increases according to the number of the flashover shocks and the increases the surface current value (see Fig. 18). The decrease in the surface current value during the rest period shown in Fig. 19 is due to the charge dissipation phenomenon. In fact, the lifetime of these charges on the insulator surface depends on the dissipation process involved such as the surface conductivity [32]-[34].

X. Meng et al [35] show that the accumulation of the surface charges on a solid insulator increases with the insulating material relative permittivity. Such accumulation of the charges which on the material surface reduces the insulator FOV, is in agreement with X. Meng et al. and our previous work [36] i.e FOV decreases with an increase in the material relative permittivity.

4 CONCLUSION

The aim of the paper is to improve our understanding of the flashover phenomenon occurring on polluted and unpolluted composite insulator surface. The conclusions drawn from our work are the following:

- Irrespective of the used pollution deposition method (controlled or uncontrolled droplet deposition), the relation between FOV and the electric conductivity of the pollution is the same
- CA and relative permittivity of the droplet increase the electric field strength, and thus the dielectric strength of the insulator surface.
- The relative permittivity of the droplet is the most important parameter for the water droplet- polluted insulator flashover, The CA droplet plays a secondary role.
- The surface current measured after A flashover occurrence increases as a function of the number of the flashover shocks as a result of the density of the electric charges involved.

REFERENCES

- [1] El-Kishky, H., Gorur, R.S. "Electric field computation on an insulating surface with discrete water droplets", IEEE Trans. Dielectr. Electr. Insul., 1996, 3, (3), pp. 450-456
- [2] Lopes, I. J. S., Jayaram, S. H., Cherney, E. A. "A study of partial discharges from water droplets on a silicone rubber insulating surface", IEEE Trans. Dielectr. Electr. Insul., 2001, 8, (2), pp. 262-268
- [3] Sarathi, R., Mishra, Palash, Gautam, Ribhu, et al. "Understanding the influence of water droplet initiated discharges on damage caused to corona-aged silicone rubber", IEEE Trans. Dielectr. Electr. Insul., 2017, 24, (4), pp. 2421-2431
- [4] Zhu, Y., Haji, K., Otsubo, M., et al. "Electrohydrodynamic behaviour of water droplet on an electrically stressed hydrophobic surface", Journal of Physics D: Applied Physics, 2006, 39, (9), pp. 1970.
- [5] Douar, M., Beroual, A., Souche, X. "Degradation of various polymeric materials in clean and salt fog conditions: measurements of AC flashover voltage and assessment of surface damages", IEEE Trans. Dielectr. Electr. Insul., 2015, 22, (1), pp. 391-399
- [6] Swift, D. A., Spellman, C., Haddad, A. "Hydrophobicity transfer from silicone rubber to adhering pollutants and its effect on insulator performance", IEEE Trans. Dielectr. Electr. Insul., 2006, 13, (4), p. 820-829
- [7] Rowland, S. M., Lin, F. C. "Stability of alternating current discharges between water drops on insulation surfaces", J. Phys. Appl. Phys., 2006, 39, (14), pp. 3067-3076
- [8] Aouabed, F. "Contribution à l'étude et à l'évaluation des performances électriques des isolations en silicone polluées sous tension alternative", Diss. Université Ferhat Abbas –Setif1, 2018.
- [9] Ndoumbe, J. "Etude comportementale des gouttelettes d'eau déposées sur la surface d'un isolateur composite haute tension en présence du champ électrique" Diss. Ecole Centrale de Lyon, 2014.
- [10] Nazemi, M. H., "Experimental investigation on water droplets on polymeric insulating surfaces under the impact of high electric fields" Diss. 2016.
- [11] Wu, X., Cao, B., Li, Z., Yang, D., Shen, S., Wang, L. "DC Breakdown Characteristic of Air Gap With Water Droplets", IEEE Trans. Plasma Sci., 2021, 49, (6), pp. 1962-1968
- [12] Nazemi, M., Hinrichsen, V. "Experimental investigations on partial discharge characteristics of water droplets on polymeric insulating surfaces at AC, DC and combined AC-DC voltages" IEEE Trans. Dielectr. Electr. Insul. 2015, 22, (4), pp. 2261-2270
- [13] Zhu, Y., Otsubo, M., Honda, C., Tanaka, S. "Corona discharge from water droplet on electrically stressed polymer surface". Japanese journal of applied physics, 2006, 45, (1R), pp. 234-238
- [14] Gao, H., Jia, Z., Mao, Y., Guan, Z., Wang, L. "Effect of Hydrophobicity on Electric Field Distribution and Discharges along Various Wetted Hydrophobic Surfaces" IEEE Trans. Dielectr. Electr. Insul, 2008, 15, (2), pp 435-443
- [15] GUAN, Z, WANG, L, YANG, B, Liang, X., Li, Z. "Electric field analysis of water drop corona. IEEE Transactions on power delivery, 2005, 20, (2), pp. 964-969.
- [16] Aouabed, F., Bayadi, A., Rahmani, A. E., Boudissa, R. "Finite element modelling of electric field and voltage distribution on a silicone insulating surface covered with water droplets". IEEE Trans. Dielectr. Electr. Insul, 2018, 25, (2), pp. 413-420
- [17] Zhu, Y., Otsubo, M., Honda, C., Hashimoto, Y., Ohno, "A. Mechanism for change in leakage current waveform on a wet silicone rubber surface-a study using a dynamic 3-D model" IEEE Trans. Dielectr. Electr. Insul, 2005, 12, (3), pp. 556-565
- [18] Abed, M. El-A, Hadi, H., Belarbi, A.W., Slama, M. El-A. "Experimental characterization of electric power insulator subjected to an accelerated environmental ageing". Elektrotehniski Vestnik, 2020, 87, (4), pp. 183-192
- [19] Ouled Ghouth, C., Si Salah, H, " Etude expérimentale des performances d'un isolateur en composite silicone soumis à différentes conditions de pollution". Université des sciences et de la technologie d'Oran, 2014
- [20] Li, Y., Zhang, X., Gao, S., Tang, X., Li, P., Li, Y., Wu, G. "Effect of Water Droplets on the Corona Discharge Characteristics of Composite Insulators in Arid Areas". 2nd Int. Conf. on Electrical Materials and Power Equipment (ICEMPE), 2019, pp. 467-472
- [21] Xing, Z., Li, C., Zhang, C., Zhang, Z., Li, W., Ru, J., Chen, X. "Influence of epoxy insulating materials parameters on surface charge characteristics and surface flashover under DC". 1st International Conference on Electrical Materials and Power Equipment (ICEMPE), 2017, pp. 184-187
- [22] Takuma, T., Techaumnat, B. "Electric Fields in Composite Dielectrics and their Applications". Springer Science & Business Media, 2010
- [23] Zhijin, Z., Tian, L., Xingliang, J., Chen, L., Shenghuan, Y., Yi, Z. "Characterization of Silicone Rubber Degradation Under Salt-Fog Environment With AC Test Voltage", 2019, IEEE Access, vol. 7, pp. 66714-66724
- [24] Morishige, Y., Suzumori, K., Wakimoto, S., Kanda, T. "Contact angle of water droplet on deforming rubber sheet with micro surface structures". IEEE/SICE International Symposium on System Integration (SII), 2015, pp. 948-951
- [25] Slama, M. El-A., Abed, M. El-A, Hadi, H., Mihoub, D., Zelmat, A., "HVAC parametric study and numerical calculation of partial discharge inception of water droplet at the surface of hydrophobic insulator", 2014, 14, (3), pp. 247-253
- [26] IEC TS 62073 "Guidance on the measurement of wettability of insulator surfaces", 2003
- [27] Abed, M. El-A. "Contribution à l'étude du vieillissement des isolateurs composites" Diss. Université des sciences et de la technologie d'Oran, 2021.
- [28] Waluyo, P. Pakpahan, et Suwarno, "Influences of Water Droplet Size and Contact Angle on the Electric Field and Potential Distributions on an Insulator Surface", IEEE 8th Int. Conf. on Properties and applications of Dielectric Materials, Bali, Indonesia, juin 2006, pp. 889-892
- [29] Fujii, O., Honsali, K., Mizuno, Y., Naito, K. "A basic study on the effect of voltage stress on a water droplet on a silicone rubber surface". IEEE Trans. Dielectr. Electr. Insul., 16, (1), pp.116-122.
- [30] Sarang, B., Basappa, P., Lakdawala, V., & Shivaraj, G. "Electric field computation of water droplets on a model insulator". Electrical Insulation Conference (EIC), 2011, pp. 377-381
- [31] Bashir, N., Ahmad, H. "Ageing of transmission line insulators: The past, present and future". IEEE 2nd International Power and Energy Conference, December 2008, pp. 30-34
- [32] Kumara, S., Ma, B., Serdyuk, Y., Gubanski, S. M. "Surface charge decay on HTV silicone rubber: Effect of material treatment by corona discharges," IEEE Trans. Dielectr. Electr. Insul., 2012, 19, (6), pp. 2189-2195
- [33] Alam, S., Serdyuk, Y. V., Gubanski, S. M. "Potential decay on silicone rubber surfaces affected by bulk and surface conductivities," IEEE Trans. Dielectr. Electr. Insul., 2015, 22, (2), pp. 970-978
- [34] Kumara, S., Serdyuk, Y. V., Gubanski, S. M. "Surface charge decay on polymeric materials under different neutralization modes in air," IEEE Trans. Dielectr. Electr. Insul., 2011, 18, (5), pp. 1779-1788
- [35] Meng, X. Mei, H. Chen, C. Wang, L., Guan, Z., Zhou, J. "Characteristics of Streamer Propagation Along the Insulation Surface: Influence of Dielectric Material," IEEE Trans. Dielectr. Electr. Insul., 2015, 22, (2), pp. 1193-1203
- [36] Bendimerad, S., Acimi, M. "Phénomènes des décharges électriques glissantes à l'interface Air/Isolant solide," Université des Sciences et Technologies d'Oran Mohamed Boudiaf (USTO-MB), 2012.

Sarah BENDIMERAD received the Master degree in electrical engineering in 2012 from the “Université des Sciences et de la Technologie d’Oran Mohamed Boudiaf”, Algeria, where she is currently preparing a Doctorate thesis in electrical power engineering with the High Voltage and Electric Field Group of the “Laboratoire de Génie Electrique d’Oran”. Her research interests include flashover phenomenon of polluted insulators and electrical discharges.

Hocine HADI is a professor at the Faculty of Electrical Engineering of the University of Sciences and Technology of Oran, and the head of the High-Voltage and Electric Field Group of the Laboratoire de Génie Electrique d’Oran when he is responsible for the Post-graduate, Master and Bachelor study program in electric power system engineering. He has been involved in several research projects and, is a member of many Scientific Committees of Algerian and international conferences. His main research interests include high-voltage insulation, dielectric materials, modelling and computation of the electric field in high-voltage equipments, high-voltage testing and electric discharge applications. He is an author/coauthor of several publications, communications and technical reports.

Mohammed El Amine ABED received the Doctor’s degree in plasmas and discharges engineering in 2021 from the “Université des Sciences et de la Technologie d’Oran Mohamed Boudiaf”, Algeria. He is currently member of High Voltage and Electric Field Group of the “Laboratoire de Génie Electrique d’Oran”. His recent work focuses on ageing phenomenon of composite insulators and high voltage fuses.